The Journal of Physiology

Mechanisms of Hebbian-like plasticity in the ventral premotor – primary motor network

Andrea Casarotto[1,2], Elisa Dolfini[1,2], Pasquale Cardellicchio[1], Luciano Fadiga[1,2], Alessandro D'Ausilio[1,2] and Giacomo Koch[1,2,3]

[1] *IIT@UniFe Center for Translational Neurophysiology, Istituto Italiano di Tecnologia, Ferrara, Italy*
[2] *Department of Neuroscience and Rehabilitation, Section of Physiology, Università di Ferrara, Ferrara, Italy*
[3] *Experimental Neuropsychophysiology Lab, Fondazione Santa Lucia IRCCS, Rome, Italy*

Handling Editors: Katalin Toth & Srikanth Ramaswamy

The peer review history is available in the Supporting Information section of this article (https://doi.org/10.1113/JP283560#support-information-section).

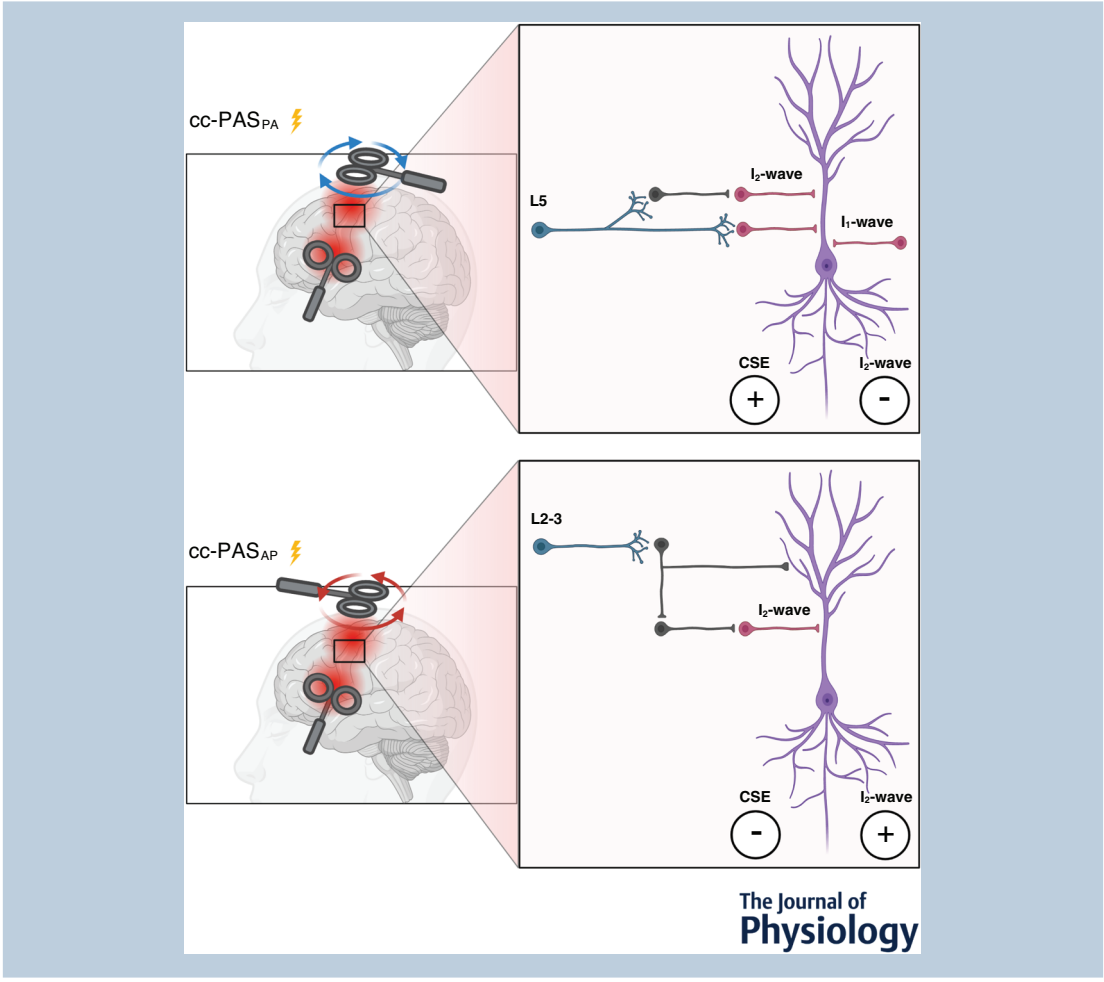

A. Casarotto and E. Dolfini contributed equally to this work.
A. D'Ausilio and G. Koch contributed as co-senior authors.

DOI: 10.1113/JP283560

Abstract The functional connection between ventral premotor cortex (PMv) and primary motor cortex (M1) is critical for the organization of goal-directed actions. Repeated activation of this connection by means of cortico-cortical paired associative stimulation (cc-PAS), a transcranial magnetic stimulation (TMS) protocol, may induce Hebbian-like plasticity. However, the physiological modifications produced by Hebbian-like plasticity in the PMv-M1 network are poorly understood. To fill this gap, we investigated the effects of cc-PAS on PMv-M1 circuits. We hypothesized that specific interactions would occur with I_2-wave interneurons as measured by the short intracortical facilitation protocol (SICF). We used different paired-pulse TMS protocols to examine the effects of PMv-M1 cc-PAS on SICF, on GABAergic circuits as measured by short (SICI) and long (LICI) intracortical inhibition protocols, and varied the current direction in M1 to target different M1 neuronal populations. Finally, we examined the effects of cc-PAS on PMv-M1 connectivity using a dual coil approach. We found that PMv-M1 cc-PAS induces both a long-term potentiation (LTP)- or long-term depression (LTD)-like after-effect in M1 neuronal activity that is strongly associated with a bidirectional-specific change in I_2-wave activity (SICF = 2.5 ms ISI). Moreover, cc-PAS induces a specific modulation of the LICI circuit and separately modulates PMv-M1 connectivity. We suggest that plasticity within the PMv-M1 circuit is mediated by a selective mechanism exerted by PMv on M1 by targeting I_2-wave interneurons. These results provide new mechanistic insights into how PMv modulates M1 activity that are relevant for the design of brain stimulation protocols in health and disease.

(Received 4 July 2022; accepted after revision 18 October 2022; first published online 3 November 2022)
Corresponding author Giacomo Koch: Department of Neuroscience and Rehabilitation, Section of Physiology, Università di Ferrara, Via Fossato di Mortara, 17–19, 44121 Ferrara, Italy. Email: giacomo.koch@unife.it

Abstract figure legend The neural circuits involved in plasticity induction after the ventral premotor cortex to primary motor cortex (PMv-to-M1) cortico-cortical paired associative stimulation (cc-PAS). Left, the cc-PAS coil orientations: postero-anterior (PA) and antero-posterior (AP). Right blocks show the neural circuits preferentially activated by the different coil orientations. The pyramidal neuron (PN) (purple) receives both excitatory (red) and inhibitory (grey) synaptic inputs responsible for the generation of I_2-waves. The PMv projections (light blue) contact the interneurons within M1 in both layers 2–3 (L2–3) and in L5. The cc-PAS_{PA} protocol preferentially target the deep neuron populations in L5, increasing the corticospinal excitability (CSE) and inhibiting the I_2-wave circuits (top block). On the other side, AP stimulation activates the more superficial neuronal populations in L2–3, inhibiting the dendritic arbour of the PN, leading to a reduction of CSE and a simultaneous increase in the activity of the I_2-wave circuit (bottom block).

Key points

- The I_2-wave is specifically modulated by the induction of ventral premotor cortex – primary motor cortex (PMv-M1) plasticity.
- After PMv-M1 cortico-cortical paired associative stimulation (cc-PAS), corticospinal excitability correlates negatively with I_2-wave amplitude.
- Different cc-PAS coil orientations can lead to a long-term potentiation- or long-term depression-like after-effect in M1.

Andrea Casarotto studied Neuroscience and Neuropsychology at the University of Bologna. Currently he is a PhD student in Neuroscience at the University of Ferrara under the supervision of Prof. Alessandro D'Ausilio and Professor Giacomo Koch. His research interests are centred on non-invasive brain stimulation and on the neurophysiological and behavioural effect of cortical plasticity induction. **Elisa Dolfini** received her PhD in Neuroscience at the University of Ferrara, under the mentorship of Professor Alessandro D'Ausilio and Professor Luciano Fadiga. There she specialized on the use of transcranial magnetic stimulation, studying the neurophysiological and behavioural inhibitory mechanisms during the joint action coordination. Currently, she is continuing her research activity on the analysis of brain connectivity.

Introduction

Human goal-directed actions are guided by a parieto-frontal network in which the ventral premotor cortex (PMv) represents a critical hub (Bencivenga et al., 2021; Fogassi et al., 2001; Grol et al., 2007; Murata et al., 1997; Raos et al., 2006; Turella & Lingnau, 2014; Umilta et al., 2007). The Parieto - PMv – M1 network is crucial in transforming object properties (e.g. size, shape and texture) into appropriate grasping actions (Davare et al., 2010; Murata et al., 1997, 2000).

Dual-site transcranial magnetic stimulation (ds-TMS) at rest shows that the PMv exerts either an inhibitory or an excitatory influence on M1, depending on the intensity of PMv stimulation (Bäumer et al., 2009; Beukelaar et al., 2016; Davare et al., 2008). This influence is also relevant during action preparation or action observation (Beukelaar et al., 2016; Davare et al., 2008; Koch, Versace et al., 2010).

Input from the PMv probably interacts with a specific set of interneurons located in M1. In monkeys, when a single stimulus delivered to F5 (homologous of PMv) conditioned a test M1 stimulus, the late indirect (I) waves of the resulting corticospinal volley are selectively facilitated (Cerri et al., 2003; Shimazu et al., 2004). In humans, the I-wave interactions during grasping preparation (Cattaneo et al., 2005) show a selective grasp-related activation of the late I_2-wave prior to movement onset, confirming that this specific circuit mediates the functional input from PMv.

Recently, cortico-cortical paired associative stimulation (cc-PAS) has been used to modulate PMv-M1 functional connectivity (Buch et al., 2011; Fiori et al., 2018). cc-PAS is a ds-TMS protocol thought to promote Hebbian spike-timing-dependent plasticity (STDP) (Hebb, 1949; Markram et al., 2011). The cc-PAS protocol mimics the neuronal pre- and postsynaptic coupling pattern that induces STDP, via a series of TMS pairs on two interconnected areas with a specific interstimulus interval (ISI). Strengthening of PMv-M1 connectivity appears to lead to a larger inhibitory influence exerted by the PMv on M1, at rest. At the same time, during action preparation, the excitatory influence exerted by the PMv is also increased (Buch et al., 2011).

However, the physiological modifications produced by cc-PAS in the PMv-M1 network and in the M1 intracortical circuitry are poorly understood.

To investigate the effect of PMv-M1 plasticity induction on the PMv-M1 circuit and M1 local circuitry, we measured the impact of the cc-PAS protocol on different M1 intracortical circuits. We hypothesized an influence of cc-PAS in specific circuits mediating the input from M1: in particular, in those with a specific interaction with I_2-wave interneurons (Cattaneo et al., 2005). We evaluated changes in short intracortical facilitation (SICF) and the effects on GABAergic interneurons by measuring short-interval intracortical inhibition (SICI; 1 and 3 ms) and long-interval intracortical inhibition (LICI; 100 ms). In another set of experiments, we explored whether PMv-to-M1 cc-PAS would also modulate PMv-M1 connectivity. In a fourth experiment, we varied the current direction (postero-anterior or PA and antero-posterior or AP) of M1 stimulation during cc-PAS, hypothesizing opposite long-term potentiation (LTP)- or long-term depression (LTD)-like after-effects due to the activation of different synaptic inputs to the corticospinal neurons (Federico & Perez, 2017; Koch et al., 2013; Ni, Gunraj et al., 2011). Indeed, while PA stimulation activates neurons in deep M1 layers, AP is more likely to stimulate superficial layers (Koch et al., 2013; Sommer et al., 2013).

Methods

Ethical approval

All the participants were informed about the experimental procedure and gave their written consent according to the last update of the *Declaration of Helsinki*, except for the registration in a database. The experiment was approved by the ethics committee 'Comitato Etico Unico della Provincia di Ferrara' (approval No. 170 592). The participants were compensated for their participation with €30.00 for their first TMS session and €15.00 if they took part in one of the subsequent experimental sessions.

Participants

A total of 39 healthy (mean age = 26 years; SD = 4.5; males: 17) volunteers took part in the study: 14 participants completed the first experimental session (*Experiment 1*); 22 subjects took part in the second experimental session (*Experiment 2, Experiment 3*); 17 subjects were recruited for the third experimental session (*Experiment 4*) and 10 subjects completed the fourth experimental session (*Experiment 5*). In the second session, due to technical problems with data acquisition, 21 participants completed *Experiment 2* while 18 completed *Experiment 3* (see Table 1).

Electromyography recording

Surface electromiography (EMG) was recorded from the right first dorsal interosseous (FDI) muscle by means of a wireless system (Zerowire EMG, Aurion, Italy) with a tendon-belly montage. EMG signals were digitized (2 kHz) and acquired with a CED Power1401-3A board (Cambridge Electronic Design, Cambridge, UK). All the acquired data were stored for offline analysis using

Table 1. For each experiment, the number of subjects, their age and rMT (mean ± SD)

Experiment	Subjects (males)	Age (years)	M1 rMT_{PA} 70 mm coil	M1 rMT_{PA} 50 mm $coil_1$	M1 rMT_{PA} 50 mm $coil_2$	M1 rMT_{AP}
1	14 (9)	27.3 ± 4.7	49.1 ± 8.8	44.8 ± 8.1	46.9 ± 8.7	
2	21 (6)	26.4 ± 4.5	47 ± 7.7	42.4 ± 7.8	44.3 ± 7.7	
3	18 (5)	26.9 ± 4.6	47.1 ± 7.1	42.5 ± 7.8	44.5 ± 7.5	
4	17 (8)	25.4 ± 5.3	47.5 ± 7.3	41.2 ± 6.7	44.4 ± 7.2	50.6 ± 7.3
5	10 (5)	25.1 ± 4.5	54.2 ± 10.1	46.5 ± 9.6	50 ± 10.7	

The rMT value indicates the percentage of the maximum stimulator output and is reported for all coils used. During the cc-PAS protocol and acquisition of connectivity, the 50 mm $coil_1$ was positioned on M1 while the 50 mm $coil_2$ was on PMv.

the Signal 3.09 software (Cambridge Electronic Design, Cambridge, UK).

TMS

Participants were seated on a comfortable armchair, during all experimental sessions, with their right arm on an armrest. They remained relaxed and they did not observe any videos or perform any actions. Single-pulse and paired-pulse TMS protocols were administered through a 70 mm figure-of-eight focal coil connected to a Magstim BiStim^2 monophasic stimulator (The Magstim Company, Whitland, UK). By contrast, for the cc-PAS protocols and PMv-M1 connectivity evaluations we used two 50 mm figure-of-eight focal coils connected to the same Magstim BiStim^2 monophasic stimulator.

The FDI optimal scalp position (OSP) was found by moving the coil in 0.5 cm steps over the left M1 hand area and using a slightly suprathreshold stimulus. Resting motor threshold (rMT) was defined as the lowest intensity that evoked a motor-evoked potential (MEP) with >50 μV amplitude in 5 out of 10 consecutive trials while the participants kept the FDI muscle relaxed (Rossi et al., 2009; Rossini et al., 2015). Table 1 gives a summary of the rMT in each experiment and coil. The individual OSP and rMT were defined for each coil used in each experiment (50 or 70 mm) and separately for the different coil orientations as later specified in the description of each experiment.

cc-PAS. In the cc-PAS protocol, dsTMS repeatedly activates the connection between left PMv and left M1. One-hundred pairs of pulses were delivered at a frequency of 0.25 Hz for ∼6 min. The left PMv was stimulated at 90% of individual rMT while the left M1 was stimulated at 120% of rMT (Koch et al., 2013). In each pair, M1 stimulation followed the PMv stimulation by 6 ms (Davare et al., 2008, 2009; Koch, Versace et al., 2010). The coil over the left M1 was placed tangentially to the scalp on the FDI OSP, at ∼45° with respect to the midline, to induce a PA current flow (*Experiment 1-2-3-5*); from this position the coil was rotated 180° to induce an AP current flow (*Experiment 4*). To estimate the position of the left PMv we used the SofTaxic Navigator System (Electro Medical System, Bologna, Italy). The skull landmarks (nasion, inion, right, and two preauricular points) and 23 points on the scalp were digitized through a Polaris Vicra optical tracker (Northern Digital, Waterloo, Canada). To stimulate the left PMv, the coil was placed over a scalp region corresponding to Montreal Neurological Institute (MNI) coordinates: $x = -52.8$, $y = 11.6$, $z = 25.1$ (Koch, Versace et al., 2010).

Neurophysiological indices

Motor-evoked potential. MEPs were collected with a single pulse protocol (sp-TMS) with a suprathreshold stimulus at 120% of the individual rMT. The amplitude of the MEP provides a global readout of corticospinal excitability (CSE) (Aguiar & Baker, 2018; Derosiere et al., 2020). Short-interval intracortical inhibition at 1 and 3 ms. SICI is measured via a paired-pulse (pp-TMS) paradigm with a first subthreshold conditioning stimulus (CS) followed, 1–5 ms later by a second suprathreshold test stimulus (TS). Here we set the CS at 80% and the TS at 120% of individual rMT. We tested two different ISIs, 1 and 3 ms, since previous studies suggest the existence of two phases, or two inhibition peaks, respectively at 1 ms and at 2.5–3 ms (Cardellicchio et al., 2021; Fisher et al., 2002; Hannah et al., 2020; Roshan et al., 2003; Vucic et al., 2011). Pharmacological studies suggest that SICI at 3 ms ISI reflects GABAa receptor-mediated fast intracortical inhibition in M1 (Di Lazzaro, Pilato, Dileone et al., 2006; Ziemann, Lönnecker et al., 1996, 2015). In particular, it has been proposed that it may represent short-lasting IPSPs in corticospinal neurons (Ilić et al., 2002; Ziemann et al., 2015). In contrast, the origin of SICI at 1 ms is still debated. Some authors propose that it does not derive from inhibitory synaptic input, but rather originates from the axonal refractoriness of neurons

recruited by the CS (Fong et al., 2021; Hannah et al., 2020), whereas others suggest that it originates from synaptic mechanisms (Fisher et al., 2002; Roshan et al., 2003).

Long-interval intracortical inhibition at 100 ms. LICI is measured via a pp-TMS paradigm consisting of two suprathreshold stimuli; the MEPs elicited by the TS (second pulses) are inhibited by the CS (first pulses). We set both the CS and the TS at 120% of the individual rMT with an ISI of 100 ms. It has been proposed that the LICI reflects $GABA_b$ receptor-mediated slow inhibition in M1 (McDonnell et al., 2006; Ziemann et al., 2015) and, in particular, slow IPSPs (Werhahn et al., 1999).

Intracortical facilitation (ICF) at 15 ms. Here ICF was elicited by a pp-TMS protocol where the CS was set at 80% and the TS at 120% of the rMT, with an ISI of 15 ms. This protocol normally shows a facilitation, which is believed to be mediated by NMDA glutamatergic receptors (Schwenkreis et al., 2000; Ziemann et al., 1998). This effect seems to reflect the activity of a circuit, at least in part, distinct from that responsible for the SICI (Ziemann, Rothwell et al., 1996, 2015).

Short-interval intracortical facilitation (SICF). To study changes in M1 intracortical circuits that are thought to receive direct input from PMv, we measured the SICF (Cattaneo et al., 2005; Di Lazzaro et al., 2012; Koch, Versace et al., 2010). The SICF was obtained by a pp-TMS protocol, with the first stimulus at 120% followed by a second stimulus at 80% of the rMT, with 1.3, 2.5 and 4.1 ms ISIs. When a TMS pulse is applied over M1, it produces a repetitive discharge of the corticospinal neurons, resulting in a series of descending volleys called 'waves'. The first, called 'direct-wave' (D-wave), results from direct activation of corticospinal neurons. The subsequent descending discharges, called 'indirect-waves' (I-waves), appear to depend on trans-synaptic excitation of intracortical interneurons that project to the corticospinal neurons (Amassian & Stewart, 2003; Di Lazzaro et al., 2012; Ziemann, 2020). Later I-waves reveal cortico-cortical pathways targeting M1, and an ISI of 2.5 ms corresponds to the peak of the I_2-wave that probably reflects inputs from the premotor cortex (Cattaneo et al., 2005; Di Lazzaro, Pilato et al., 2006, 2012; Shimazu et al., 2004). The resulting facilitation is produced because the peaks of the I-waves evoked by the two subsequent pulses are in phase (Di Lazzaro et al., 2012; Federico & Perez, 2017).

Connectivity protocol

The ds-TMS protocol is a well-established method to assess the functional connectivity between brain sites. A first CS was delivered over PMv to activate the projections towards M1 followed by TS over M1, 6 ms later (Davare et al., 2008, 2009; Koch, Versace et al., 2010). However, previous studies suggest that different CS intensities over the premotor cortex may induce either a facilitatory or an inhibitory influence on M1 (Bäumer et al., 2009; Davare et al., 2008). These opposite effects may be due to activation of different neuronal populations. Here we used different CS intensities (30, 50, 70 and 90% of the individual rMT) and a fixed TS intensity set at 120% of the rMT.

Experimental procedure

Experiment 1: effect of PMv-to-M1 cc-PAS_{PA} on M1 neurophysiological indexes (n = 14). To investigate the neurophysiological modifications induced by conditioning the PMv-to-M1 connectivity, we collected different excitatory and inhibitory indices before and after the cc-PAS protocol. More specifically, we measured the MEP, LICI, SICI (with an ISI of 1 and 3 ms), ICF and SICF (only at an ISI of 2.5 ms). A total of 120 trials were collected, that is 20 repetitions for each index. Previous work has shown how the LICI protocol influences subsequent SICI acquisition (Ni, Gunraj et al., 2011) while it does not interact with ICF. The LICI protocol was administered 100 ms before the SICI/ICF. In the present study, all indexes were acquired in a randomized order to avoid order effects and with an interval of 5 s to avoid carryover effects between the different protocols. All indexes were acquired before the cc-PAS protocol as well as 10 min (post-10) and 30 min (post-30) after the end of the cc-PAS protocol (see Fig. 1).

Experiment 2: SICF modulations induced by PMv-to-M1 cc-PAS_{PA} (n = 21). To investigate if the reduction observed in the SICF (*Experiment 1*) was specific for the tested ISI (2.5 ms), we measured the SICF before and after the PMv-to-M1 cc-PAS protocol with different ISIs. Specifically, we used 1.3, 2.5 and 4.1 ms ISIs, which correspond to the timing of the different I-waves (Cattaneo et al., 2005). At the same time, we also tested the 2.1and 3.3 ms ISIs, which do not target specific I-waves and offer a clear baseline, beside the single-pulse MEPs (Cattaneo et al., 2005). A total of 60 trials were collected, 10 for each condition. All the conditions were randomized within each block. All measures were obtained before the cc-PAS protocol and 30 min later (post-30; Fig. 1).

Experiment 3: connectivity modulation induced by PMv-to-M1 cc-PAS_{PA} (n = 18). We investigated the modification induced by the PMv-to-M1 cc-PAS protocol on the connectivity between left PMv and M1. We explored different CS intensities (30, 50, 70 and 90% of the individual rMT) as well as single-pulse MEPs as a reference condition. Ten trials for each condition

were acquired, for a total of 50 trials. All the conditions were randomized within each block. All measures were obtained before the cc-PAS protocol and 30 min later (post-30; Fig. 1).

Experiment 4: effects of PMv-to-M1 cc-PAS$_{AP}$ on M1 neurophysiological indexes and PMv-M1 connectivity (n = 17). In this experiment, we changed the direction of the induced current over M1 during the cc-PAS protocol from PA to AP. The cc-PAS protocol was applied as reported in *Experiment 1* except that the coil over M1 was rotated 180° to induce an AP current (M1: 120% of FDI rMT$_{AP}$; PMv: 90% of FDI rMT$_{PA}$). We recorded the MEPs and the SICF (2.5 ms ISI). We also measured the connectivity between PMv and M1 by using two CS intensities over PMv (30 or 70% of rMT$_{PA}$) while the TS over M1 was applied at 120% of rMT$_{PA}$ with the coil in PA orientation. Fifteen trials were collected for each measure. All measures were obtained before the cc-PAS protocol and 30 min later (post-30; Fig. 1).

Experiment 5: M1-to-PMv cc-PAS$_{PA}$ (n = 10). The aim of this experiment was to evaluate if the modulations observed in M1 intracortical circuits were specific for the conditioning exerted by PMv onto M1. The cc-PAS protocol was administered as reported in the TMS section above but now the M1 stimulation preceded the left PMv stimulation by 6 ms. The coil over M1, FDI hotspot, was positioned with PA orientation. Fifteen trials were collected for each measure, MEPs and the SICF (ISI of 2.5 ms), before and 30 min after the cc-PAS protocol (see Fig. 1).

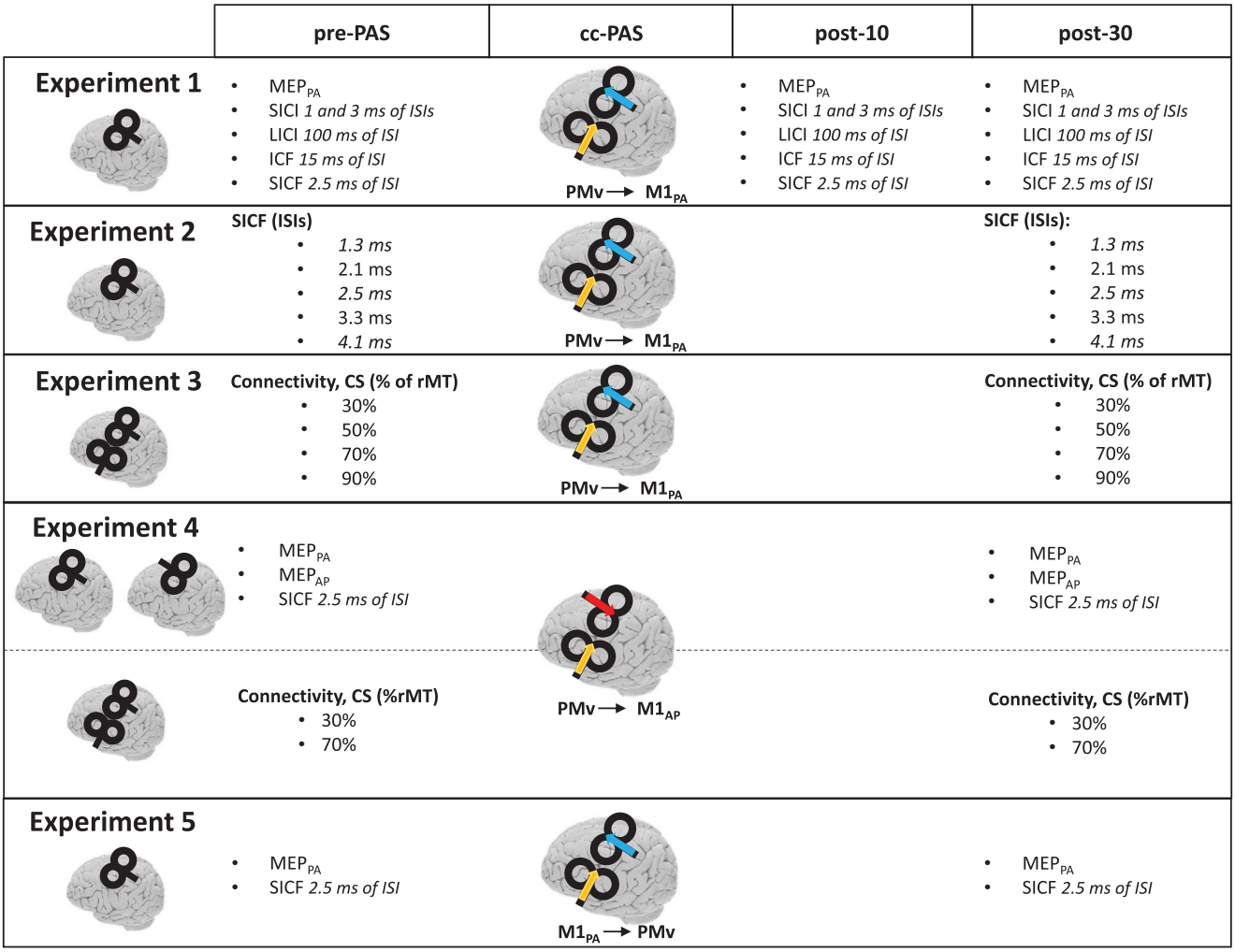

Figure 1. Table summarizing all experimental procedures
cc-PAS was preceded by the baseline acquisition (pre-PAS) and followed by the reacquisition (post-10 and post-30) of the same indices to evaluate the modulation caused by the plasticity-inducing protocol. For each experiment, the first column specifies the coil position for the acquired indices, while the cc-PAS column shows the coil position for the cc-PAS administration and the induced current direction (arrows).

Analysis and results

We excluded from the analysis all trials that presented a peak-to-peak MEP amplitude ≤0.05 mV. Moreover, for each subject we calculated the mean and standard deviations of the background pre-TMS EMG (100 ms) over all trials. We removed from the analysis those trials that presented a pre-trigger EMG activity exceeding the mean by 2 SD. All trials were visually inspected for artefacts. All analyses were conducted on STATISTICA 12 (StatSoft, Inc., Tulsa, OK, USA). Finally, although approximately 2 weeks elapsed between experimental sessions, we analysed the MEPs recorded in 13 participants who took part in one or more sessions to avoid any interference effects. No significant differences were found between these groups ($t_{13} = 0.02$; $P = 0.96$).

Data treatment

MEPs amplitudes are given in millivolts. Neurophysiological indices based on pp-TMS (ICF, SICI and SICF) are expressed as the ratio between their mean MEP amplitude and the mean MEP size in the sp-TMS protocol. The LICI, by contrast, is expressed as the ratio between the TS and CS amplitudes in every trial, to avoid modulations driven by local excitability changes in M1. In *Experiments 3* and *4* connectivity (ds-TMS) is expressed as the ratio between mean MEP size (obtained when PMv was stimulated before M1) and the mean MEP amplitude obtained via the sp-TMS protocol.

Results

Experiment 1. We computed a one-way repeated-measures ANOVA with 'Time' as factor on three levels (pre-PAS/post-10/post-30), separately for each neurophysiological index. The ANOVA did not show any effect of Time for the ICF ($F_{1,13} = 0.43$; $P = 0.65$), for the SICI with an ISI of 1 ms ($F_{1,13} = 0.61$; $P = 0.54$) or for the SICI with an ISI of 3 ms ($F_{1,13} = 0.78$; $P = 0.46$). In contrast, a significant effect of Time was found for the SICF ($F_{1,13} = 5.04$; $P = 0.01$). The *post hoc* analyses, with Bonferroni correction, revealed a significant reduction of the SICF at post-10 (mean (M) = 1.21; SD = 0.18; $P = 0.03$) and at post-30 ($M = 1.21$; SD = 0.23; $P = 0.03$) with respect to the pre-PAS acquisition ($M = 1.38$; SD = 0.23). No significant difference was found between post-10 and post-30 ($P = 0.99$). The ANOVA on the sp-TMS MEPs showed a significant effect of Time ($F_{1,13} = 4.28$; $P = 0.02$). The *post hoc* analyses, with Bonferroni correction, revealed a significant CSE increment at post-30 ($M = 2.40$ mV; SD = 1.40, $P = 0.03$) compared to the pre-PAS acquisition ($M = 1.87$ mV, SD = 1.16). No significant difference was present between pre-PAS and post-10 ($M = 2.27$ mV, SD = 1.43, $P = 0.13$) or between post-10 and post-30 ($P = 0.99$). The ANOVA on LICI showed a significant effect of Time ($F_{1,13} = 4.99$, $P = 0.01$). The *post hoc* analyses, with Bonferroni correction, showed a significantly larger inhibition for post-10 ($M = 0.14$, SD = 0.11, $P = 0.03$) and post-30 ($M = 0.15$, SD = 0.14, $P = 0.04$) compared to the pre-PAS acquisition ($M = 0.29$, SD = 0.27). No significant difference was present between post-10 and post-30 ($P = 0.99$). All results are reported in Fig. 2.

We then calculated the individual relative change induced by cc-PAS on the MEP, SICF and LICI as the ratio between the post-30 and pre-PAS acquisitions. The data were then subjected to a Pearson correlation analysis to test whether a change in one index was associated with a stable change in another one. We found a significant negative correlation between the increment of the MEP ($M = 1.39$, SD = 0.46) and the reduction of the SICF ($M = 0.88$, SD = 0.15, $r = -0.62$, $P = 0.02$). No significant correlation was found between the MEP and the LICI ($M = 0.95$, SD = 0.85) modulation ($r = -0.09$, $P = 0.77$) or between the SICF and LICI modulation ($r = 0.08$, $P = 0.77$).

Experiment 2. We computed five Bonferroni-corrected paired-sample two-tailed t tests between the pre-PAS and the post-30 acquisition on the SICF data. No significant results were found for the SICF with an ISI of 1.3 ms ($t_{21} = 0.49$, $P = 0.62$) and 4.1 ms ($t_{21} = 0.39$, $P = 0.70$). In contrast, a significant reduction of the SICF was found with an ISI of 2.5 ms between pre-PAS ($M = 1.3$, SD = 0.30) and post-PAS acquisition ($M = 1.11$, SD = 0.32) ($t_{21} = 2.98$, $P = 0.007$). No significant modulations were found for an ISI of 2.1 ms ($t_{21} = -0.44$, $P = 0.66$) or 3.3 ms ($t_{21} < 0.0001$, $P = 0.99$). We replicated and extended the previous result, obtained in *Experiment 1*, on the SICF. Indeed, the reduction of the SICF was specific for the ISI of 2.5 ms. The results are reported in Fig. 3.

Experiment 3. We first evaluated the connectivity between PMv and M1 before cc-PAS with four Bonferroni-corrected one-sample two-tailed t tests, between the conditioned MEP (pp-TMS with different stimulation intensities on PMv followed by a constant stimulus intensity on M1), and the sp-TMS protocol. No significant difference was found when the PMv was stimulated at 30% ($t_{18} = -0.18$, $P = 0.86$), 50% ($t_{18} = -0.81$, $P = 0.43$) or 90% of the rMT ($t_{18} = -0.12$, $P = 0.91$). When the CS on the PMv was set at 70% of the rMT, the MEPs were significantly reduced ($M = 1.91$, SD = 1.30, $t_{18} = -3.33$, $P = 0.007$).

We then evaluated if the cc-PAS modulated the PMv-M1 connectivity by comparing the conditioned MEPs before (pre-PAS) and after (post-30), through

four two-tailed paired-sample *t* tests, with Bonferroni correction. No significant modulation on the connectivity was found when the CS on PMv was at 30% ($t_{18} = -0.38$, $P = 0.71$), 50% ($t_{18} = -0.94$, $P = 0.36$) or 90% of rMT ($t_{18} = -0.19$, $P = 0.85$). In contrast, the inhibitory effect exerted by the PMv when the CS was set at 70% of the rMT disappeared and the difference between the pre-PAS ($M = 0.86$, SD $= 0.17$) and the post-30 ($M = 1.04$, SD $= 0.18$) was significant ($t_{18} = -3.05$, $P = 0.007$). The results are reported in Fig. 4.

Experiment 4. We first analysed MEP latencies elicited by the PA and AP TMS stimulation. A two-tailed paired-sample *t* test showed a significantly shorter latency ($t_{18} = 11.67$, $P < 0.0001$) for MEP_{PA} ($M = 21.76$ ms, SD $= 2.22$) with respect to MEP_{AP} ($M = 23.58$ ms, SD $= 1.87$). Accordingly, the different trans-synaptic set of input engaged in PA *vs.* AP should result in a constantly delayed MEP latency of about 1.5 ms (Di Lazzaro, Pilato et al., 2006; Federico & Perez, 2017; Koch et al., 2013; Ni et al., 2011a).

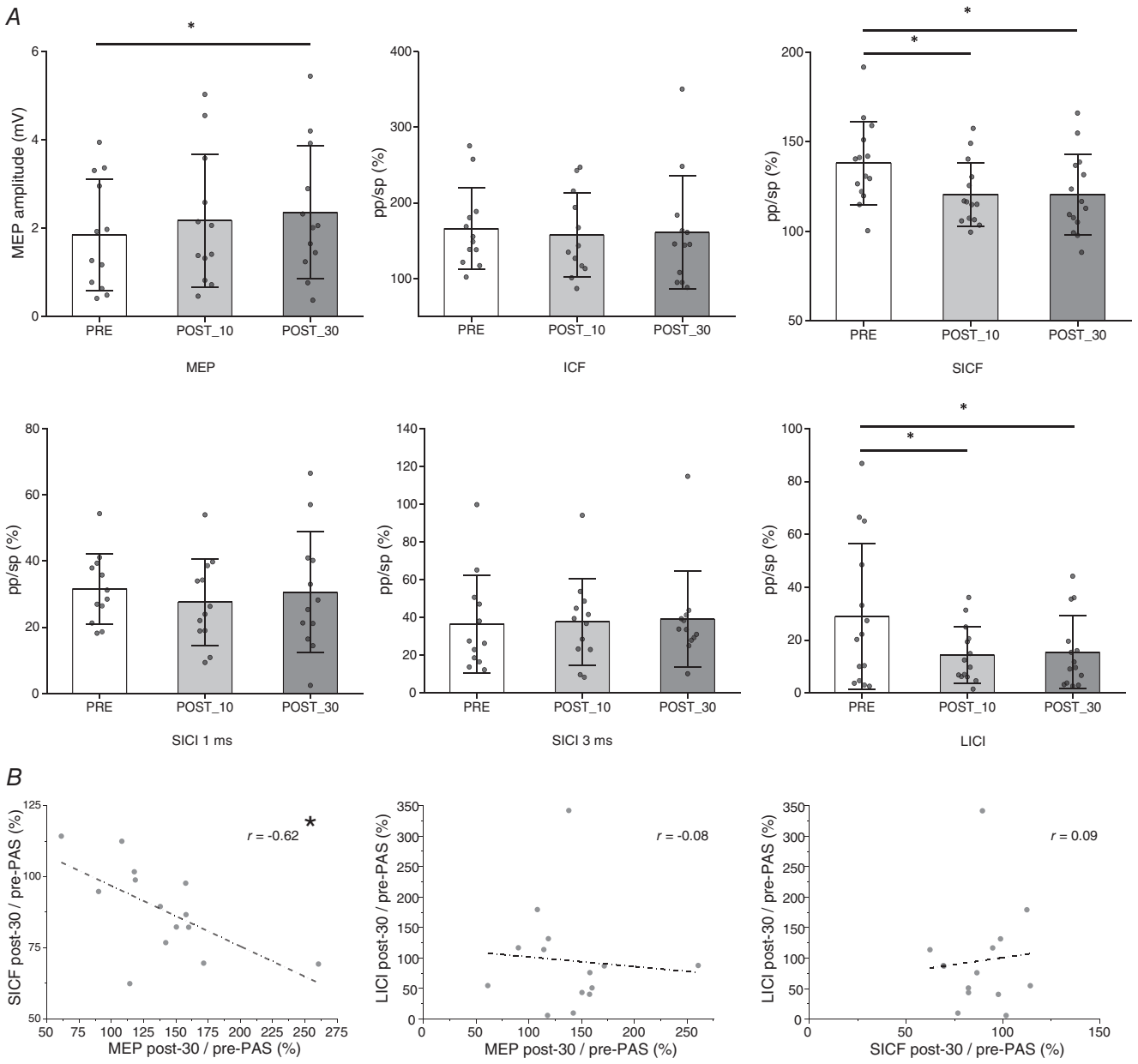

Figure 2. Results of *Experiment 1*
A, the effect of the PMv-to-M1 cc-PAS protocol on the different indices. SICI, ICF and SICF are expressed as the ratio of the mean MEP amplitude (pp-TMS/sp-TMS). The error bars on the histograms represent the standard deviation (SD). *B*, correlation results between the significantly modulated indices. $^*P < 0.05$.

Then, by means of Bonferroni-corrected paired-sample two-tailed t tests, we found a significant reduction ($t_{17} = 3.48$, $P = 0.003$) of MEP_{PA} amplitude in post-30 ($M = 1.78$ mV, SD = 1.05) compared to pre-PAS ($M = 2.14$ mV, SD = 1.12). Note that this is the opposite pattern to that seen in *Experiment 1*. At the same time, we found no significant modulation of MEP_{AP} between pre-PAS ($M = 1.17$ mV, SD = 0.70) and post-30 ($M = 1.29$ mV, SD = 1.03, $t_{17} = -0.71$, $P = 0.49$). The $SICF_{2.5ms}$ showed a significant increment ($t_{17} = -2.36$, $P = 0.03$) in post-30 ($M = 2.03$, SD = 1.74) with respect to pre-PAS ($M = 1.23$, SD = 0.69). Note that this is the opposite pattern to that seen in *Experiment 1*. As in *Experiment 1* we evaluated if there was a correlation between the modulation of MEP and the modulation of the SICF, at the individual level. We found a significant negative correlation ($r = -0.75$, $P = 0.0004$) between the reduction of the MEP_{PA} and the increment of the SICF. This is the same pattern as that seen in *Experiment 1*. The results are reported in Fig. 5.

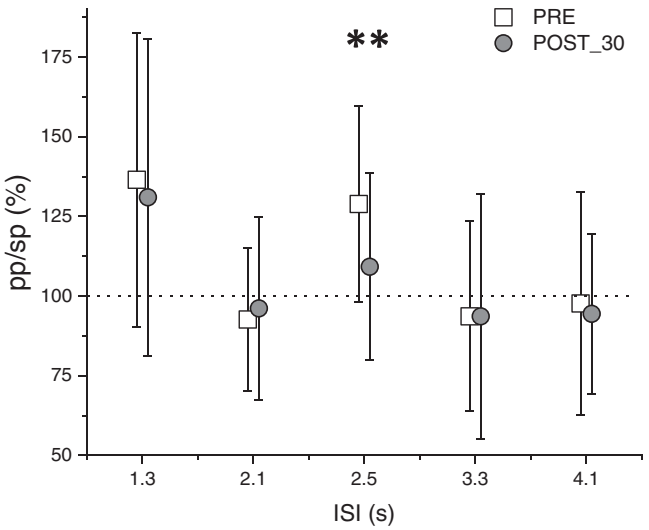

Figure 3. Results of *Experiment 2*; the effect of the PMv-to-M1 cc-PAS on the SICF at different ISIs, each reflecting different I-waves
A selective modulation of the I_2-waves is observable. The error bars represent the SD. $^{**}P < 0.01$, in a t test with Bonferroni correction for multiple comparison.

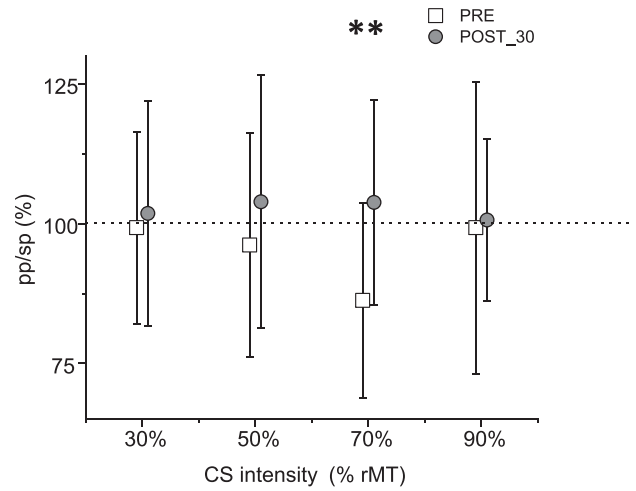

Figure 4. Results of *Experiment 3*
The PMv expressed an inhibitory influence on M1 only when it was stimulated at 70% of the rMT. This inhibitory influence was suppressed after the PMv-M1 cc-PAS protocol. The error bars represent the SD. $^{**}P < 0.01$, in a t test with Bonferroni correction for multiple comparison.

For the connectivity measures we applied the same statistical analyses used in *Experiment 3* and we replicated the results obtained in the pre-PAS acquisition of *Experiment 3*. Indeed, before the cc-PAS protocol when the PMv was stimulated at 70% of the rMT, we showed an inhibitory influence on M1 ($t_{17} = -2.81$, $P = 0.01$). However, no significant difference was found when the stimulation of PMv was set at 30% of the rMT ($t_{17} = -0.63$, $P = 0.53$). In addition, the $cc\text{-}PAS_{AP}$ effect on connectivity was the same as in *Experiment 3*. More precisely, a significant modulation of the PMv-M1 connectivity was found between the pre-PAS ($M = 0.91$ mV, SD = 0.13) and post-30 ($M = 1.04$ mV, SD = 0.19) acquisition when the PMv was stimulated at 70% of the rMT ($t_{17} = -2.65$, $P = 0.01$). No significant change was seen when PMv was stimulated at 30% of the rMT ($t_{17} = -0.41$, $P = 0.69$). The results are reported in Fig. 5.

Experiment 5. As in the control experiment, we applied cc-PAS in the opposite temporal order (M1 first). No significant modulation emerged in MEP amplitude between pre-PAS ($M = 1.83$ mV, SD = 0.68) and post-30 ($M = 1.95$ mV, SD = 0.66, $t_{10} = -0.50$, $P = 0.63$) acquisitions. In the same way, no significant modulation was found in the SICF (ISI = 2.5 ms) between the pre-PAS ($M = 1.63$, SD = 0.49) and the post-30 ($M = 1.84$, SD = 0.80, $t_{10} = -1.23$, $P = 0.25$) acquisition (Fig. 6).

Discussion

To better understand the nature of PMv-M1 connectivity modulations, we believe it is essential to investigate the neurophysiological modulations reflecting complex intracortical reorganization within M1. Here, after cc-PAS, we observed in parallel: (i) long-lasting enhanced/decreased corticospinal excitability, as indexed by MEP amplitude changes, that was strongly associated with long-lasting enhanced/decreased I_2-waves, as measured by $SICF_{2.5ms}$ amplitude change; (ii) an independent long-lasting change of LICI; (iii) a cc-PAS-induced plasticity that is dependent on current direction in M1; and (iv) modulation of the strength of PMv-M1 connectivity.

Summing up, we show that conditioning the PMv-M1 network via a cc-PAS protocol induces a clear modulation of both the PMv-M1 connectivity and selective M1 local circuitry. These modulations evolve rapidly (after 10 min) and persist for at least 30 min.

Effects of PMv-to-M1 cc-PAS corticospinal excitability

In this work we systematically explored the effects of cc-PAS in the PMv-M1 network using a ds-TMS protocol to promote Hebbian-like STDP (Hebb, 1949; Markram et al., 2011).

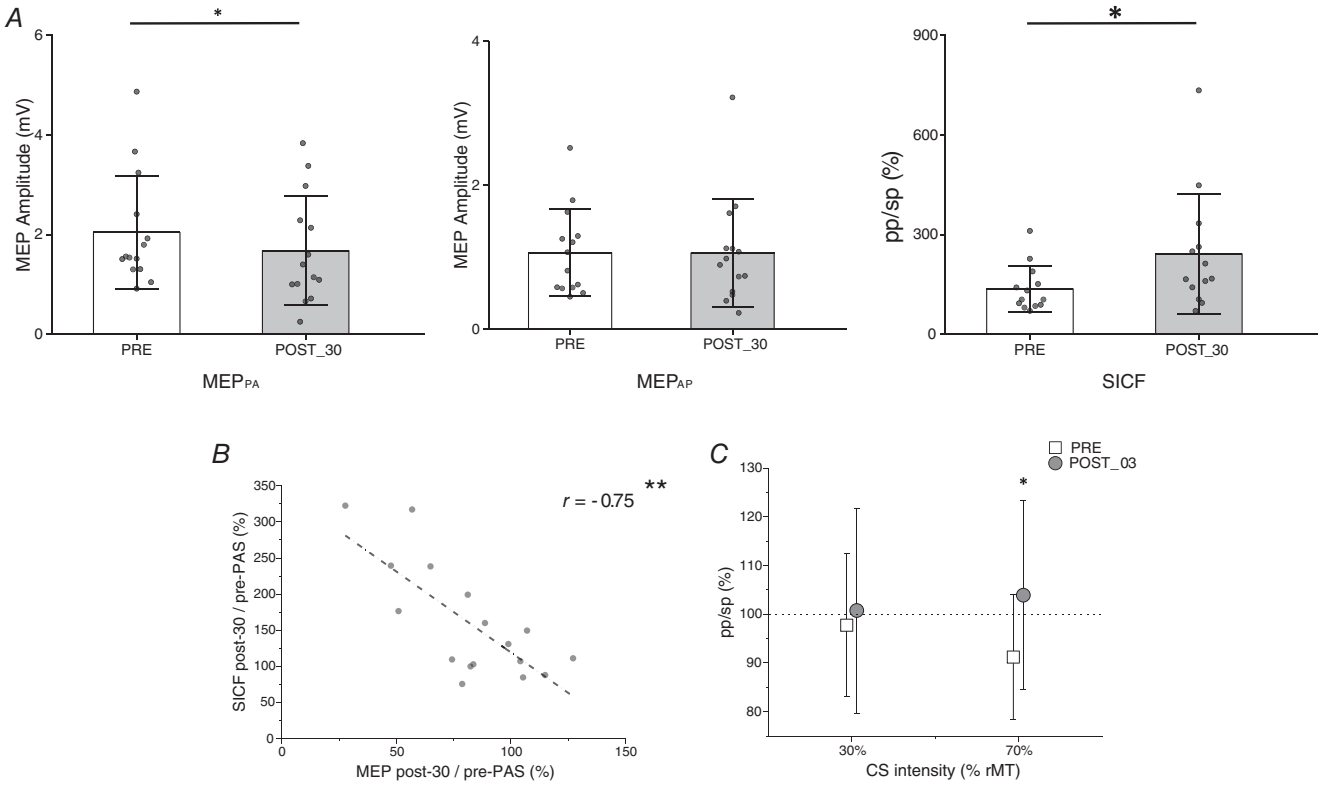

Figure 5. Results of *Experiment 4*
A, the effect of cc-PAS in AP orientation. The modulations observed in the MEP_{PA} and in the SICF are the opposite of those induced by cc-PAS in PA orientation (*Experiment 1*). *B*, correlation between the MEP_{PA} and the SICF. *C*, effect induced by cc-PAS_{AP} on the connectivity between PMv and M1. The error bars represent the SD. $^{*}P < 0.05$, $^{**}P < 0.01$.

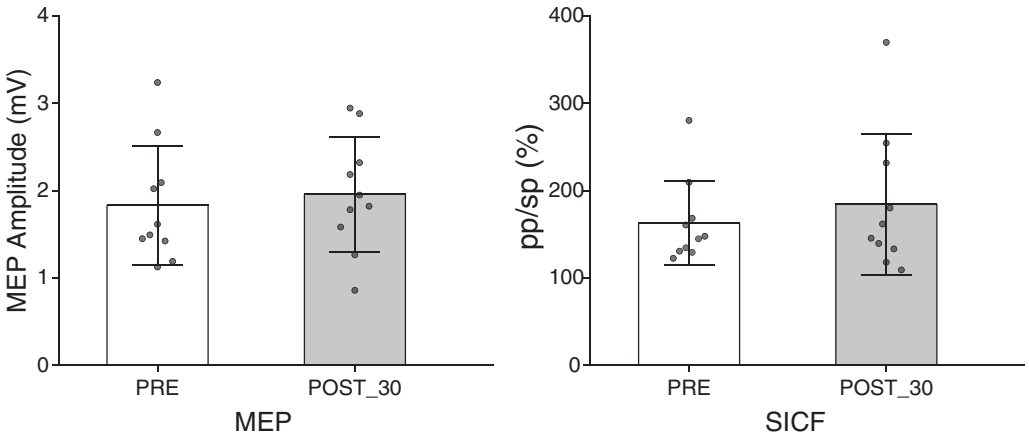

Figure 6. Results of *Experiment 5*
The M1-to-PMv cc-PAS showed no modulation of the MEP or SICF after 30 min. The error bars represent the SD.

We found that at the corticospinal level, cc-PAS led to opposite LTP-like or LTD-like after-effects depending on the coil orientation, PA *vs.* AP respectively. This result is consistent with previous observations from our group in which similar dynamics were reported in the context of the posterior parietal cortex (PPC)-M1 network (Koch et al., 2013; Veniero et al., 2013). The PA orientation preferentially targets the deeper neural layers in M1, whereas the AP orientation probably targets the more superficial layers (Koch et al., 2013; Sommer et al., 2013). Previous works have demonstrated how plasticity in M1 can depend on the relative distance between the synaptic site and the soma of the pyramidal neurons (Sjöström & Häusser, 2006). Activation of the connection from layer 2 and layer 3 (L2 and L3), in other words the connection from a more superficial neuronal population projecting far from the soma of the pyramidal neurons, leads to LTD. In contrast, activation from layer 5 (L5), which is the connection from a deeper neural population that could project near to the soma of the pyramidal neurons, leads to LTP in M1 (Kampa et al., 2007; Sjöström & Häusser, 2006).

cc-PAS$_{PA}$ might preferentially target deeper neural populations in L5 projecting near to the soma of the pyramidal neurons in M1 (Sjöström & Häusser, 2006). This may lead to the larger CSE observed in *Experiment 1* (Fig. 7*A*).

Conversely, the reduction of the CSE in *Experiment 4* (cc-PAS$_{AP}$) might be due to the preferential recruitment of superficial neuronal populations, in L2 and L3, that project far from the soma of the pyramidal neurons situated in L5 (Koch et al., 2013; Sjöström & Häusser, 2006). Indeed, it is possible that interneurons located in L2–L3 inhibit the dendritic arbour of the large pyramidal cells (Jiang et al., 2013) (Fig. 7*B*). Together, this suggests that cc-PAS delivered with PA *vs.* AP induces opposite long-lasting effects, equivalent to LTP and LTD respectively.

Effects of PMv-to-M1 cc-PAS on I_2-wave activity

In *Experiment 1*, the PMv-to-M1 conditioning protocol in the PA direction determines specific modifications of the excitatory descending volleys as early as 10 min after cc-PAS. *Experiment 2* showed that the influence of the PMv is specific to the I_2-wave (SICF$_{2.5ms}$). This result is in line with previous non-human primate data, which identified the PMv as the site of origin of inputs to M1 that contribute to the generation of the late descending I-waves (Shimazu et al., 2004). The concurrent lack of modulation observed for the first I_1-wave supports the idea of a different circuit for the generation of the I_1- and the I_2-wave (Di Lazzaro & Rothwell, 2014; Di Lazzaro et al., 2012).

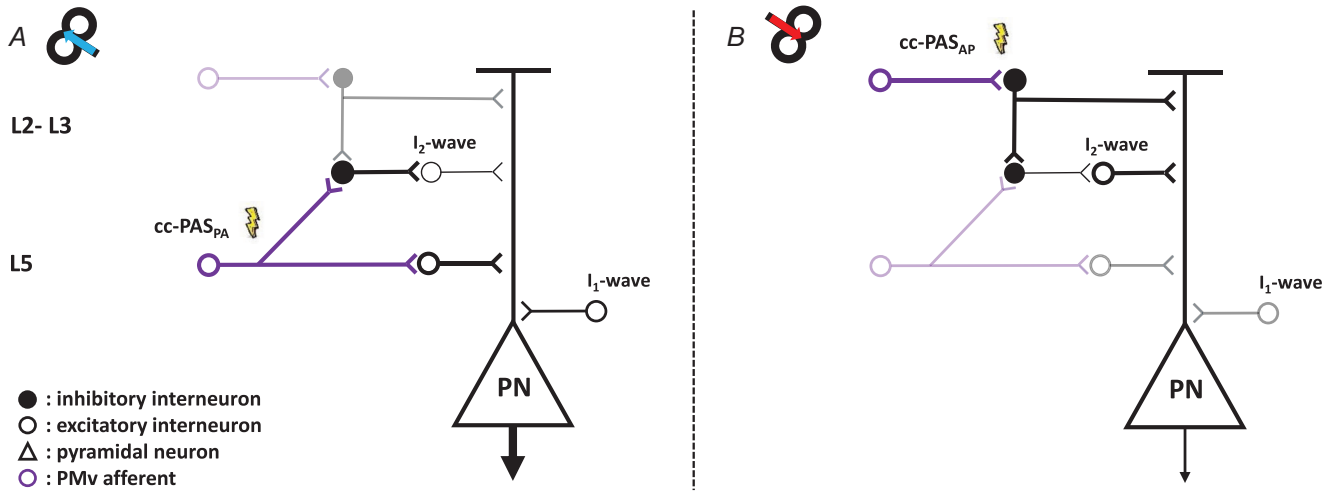

Figure 7. Model of the possible neural circuits involved in the plasticity changes after the PMv-to-M1 cc-PAS
The large pyramidal neuron (PN) in L5 of M1, which projects to the spinal cord, receives both excitatory (white circle) and inhibitory (black circle) synaptic inputs responsible for the I_2-waves. The PMv projections (violet circle) contact the interneurons both in L2–3 and in L5 of M1 (Ghosh & Porter, 1988). The lightning bolt represents the preferential activation layers of the cc-PAS stimulation while the shaded circuits indicate the not preferential action sites of cc-PAS and the thickness of neurons indicates the increase or decrease in their activity. *A*, the PMv projection that synapses with the interneurons in the deepest layer (L5), preferentially enhanced by the cc-PAS in PA direction, excites the PN, leading to an increment of the CSE, and inhibits the circuit responsible for the I_2-waves. *B*, on the other side, the more superficial interneurons populations in L2-3, probably responsible for the I_2-wave and preferentially activated by the AP stimulation, can inhibit the dendritic arbour of the PN (Jiang et al., 2013), leading to reductions of the CSE, and in parallel enhance the I_2-waves exciting the responsible circuitry.

In parallel with the reduction of the $SICF_{2.5ms}$, we showed an increase in the corticospinal excitability after the cc-PAS_{PA} protocol, as discussed above. More importantly, we found a robust negative correlation between MEP and $SICF_{2.5ms}$, which supports the idea that these two indices, although reflecting different circuits within M1, are functionally coupled at single-subject level.

To evaluate the nature of this correlation, in *Experiment 4* we applied the cc-PAS protocol in the AP direction. By changing the TMS current direction it is possible to target different synaptic inputs to the corticospinal neurons (Federico & Perez, 2017; Fong et al., 2021; Hamada et al., 2014; Koch et al., 2013; Ni et al., 2011a). The PA stimulation preferentially elicits the earliest I-waves, while the AP stimulation preferentially elicits late I-waves (Di Lazzaro & Rothwell, 2014; Ni et al., 2011a). Here, reversing the current direction from PA to AP, we confirmed the strong correlation between the MEP and the $SICF_{2.5ms}$ but with an inversion of the effects induced in *Experiment 1*. Specifically, we observed a reduction of the CSE paralleled by a larger I_2-wave ($SICF_{2.5ms}$). Finally, these modifications are specific for the cc-PAS protocol applied. When we reversed the timing, i.e. M1 stimulated 6 ms before the PMv, these effects were cancelled (*Experiment 5*).

The consistency of the correlation between CSE and I_2-waves, across different current directions, also suggests a mechanism-based on a simple circuit, formed by few interneurons, probably located in L2–L3, and differently influenced by the PMv projections to different M1 layers (Fig. 7). This correlation might reflect a fine push–pull control mechanism exerted by PMv to regulate the M1 activity state at rest or M1 output during action preparation (Johnson et al., 2012).

Based on these results, we suggest that the neuronal populations responsible of the generation of the I_2-wave ($SICF_{2.5ms}$) can differentially be inhibited or disinhibited using different cc-PAS protocols (PA *vs*. AP; Fig. 7). The robust and selective modulation of the I_2-wave indicates the $SICF_{2.5ms}$ as a preferential channel to investigate the interactions between these areas.

Although more specific studies will be needed to understand how these cc-PAS modulations could be linked to motor behaviour, previous studies have shown how both the $SICF_{2.5ms}$ (Cattaneo et al., 2005) and the CSE was increased during action preparation (Klein et al., 2012; Leocani et al., 2000; Poole et al., 2018). Federico & Perez (2017) demonstrated how less synchronized synaptic inputs, activated by AP stimulation, were preferentially recruited during the power grip. This suggests the possibility of targeting and conditioning the neural subpopulation within M1 preferentially recruited during a specific action. Future studies should investigate this opportunity and its implications for the field of motor rehabilitation.

Effects of PMv-to-M1 cc-PAS on GABAergic activity

We found that the cc-PAS protocol induced specific changes on local GABAergic interneuronal activity. Importantly, we show an dissociation between inhibitory indexes, with larger slow inhibitory activity (LICI; probably mediated by metabotropic $GABA_b$ receptors) (McDonnell et al., 2006; Werhahn et al., 1999) while the fast local one was unaltered (SICI; probably mediated by ionotropic $GABA_a$ receptors) (Ilić et al., 2002; Müller-Dahlhaus et al., 2008; Ziemann, Lönnecker et al., 1996). This result might be driven by the very nature of the cc-PAS stimulation, which is considered to produce a long-lasting potentiation. Indeed, according to Hebbian principles, a stable change in synaptic strength is driven by pre- and postsynaptic activities that, beside glutamate, can also be mediated by GABAergic metabotropic receptor pathways (Mott & Lewis, 1991). In fact, slow inhibitory control of neuronal excitability exerts its influence at both the pre- and the postsynaptic levels – presynaptically via Ca^{2+}-mediated reduction of GABA and glutamate release, and postsynaptically through robust slow K^+-mediated hyperpolarization (Dutar & Nicoll, 1988; Sanchez-Vives et al., 2021). Together, our data suggest that slow GABAergic activity might be implicated in the regulation of LTP-like mechanisms independently from the interaction with the I_2 circuits described above.

Effects of PMv-to-M1 cc-PAS on connectivity

We observed that the cc-PAS protocol changes the strength of PMv-M1 connectivity. Previous findings suggest that stimulating the PMv at different intensities recruits different projections exerting different excitatory or inhibitory influences on M1 (Bäumer et al., 2009). In particular, stimulation of the PMv at 80% or 90% of the rMT, 4–6 ms before M1, highlights an inhibitory drive to M1 (Bäumer et al., 2009; Davare et al., 2008) while stimulation at 80% of active motor threshold (aMT) produces an excitatory effect (note that 80% aMT roughly corresponds to 60–70% rMT) (Bäumer et al., 2009). In the pre-PAS acquisition, our results clearly support the intensity-dependent inhibitory influence of PMv towards M1 at rest. We find that the peak of inhibition is recruited with a stimulus intensity of 70% of the rMT. At the same time, none of the intensities explored here (30, 50, 70 and 90% of rMT) show any excitatory effect on M1.

Yet, after cc-PAS, the PMv inhibitory drive towards M1 disappeared to switch, qualitatively, to a more facilitatory influence. This effect is not intensity-dependent and, appears to be non-specific but caused by the induction of plasticity. Indeed, previous studies showed similar suppression of the influence between areas after different conditioning protocols (Koch, Cercignani et al., 2010;

Pauly et al., 2022). Moreover, measures of connectivity were not affected by current direction since we were able to replicate previous results (*Experiment 3*) also with cc-PAS_{AP} (*Experiment 4*). Consequently, the long-lasting Hebbian-like effects on PMv-to-M1 connectivity, due to the plasticity-induction protocol, is indirectly mediated by specific local M1 circuitry.

Conclusion

These data provide novel insight into the neurophysiological basis of the PMv-to-M1 cc-PAS protocol. The functional connectivity between PMv and M1 covers a key function in the visuomotor transformations necessary for goal-directed actions and, understanding how to manipulate it might become crucial for the application of cc-PAS in future research as well as in motor rehabilitation. We highlight that the PMv-to-M1 cc-PAS influences both the connectivity between these areas and the M1 local circuitry.

The modulations induced in M1 depend on the current direction induced by the stimulation. Indeed, the PA *vs*. AP stimulations appear to induce two different long-lasting effects in M1, respectively identifiable as LTP and LTD. At the same time, we found a specific modulation of the neuronal circuit responsible of the I_2-wave, highlighting PMv as the specific source of the input to M1 responsible for its generation. The selective modulations of the I_2-wave support the use of the $SICF_{2.5ms}$ as a marker of the influence of PMv on M1. Moreover, we showed a significant negative correlation between the CSE and the I_2-wave modulation. We suggest that this correlation could reflect different circuits, functionally coupled, within M1. These circuits may create a fine control mechanism, influenced by PMv, responsible of the regulations of the M1 motor output drive. Future studies will need to investigate how these neurophysiological modifications are involved in different types of movement.

References

Aguiar, S. A., & Baker, S. N. (2018). Convergent spinal circuits facilitating human wrist flexors. *Journal of Neuroscience*, **38**(16), 3929–3938.

Amassian, V. E., & Stewart, M. (2003). *Motor cortical and other cortical interneuronal networks that generate very high frequency waves*. Elsevier B.V. Available at: https://doi.org/10.1016/S1567-424X(09)70214-4

Bäumer, T., Schippling, S., Kroeger, J., Zittel, S., Koch, G., Thomalla, G., Rothwell, J. C., Siebner, H. R., Orth, M., & Münchau, A. (2009). Inhibitory and facilitatory connectivity from ventral premotor to primary motor cortex in healthy humans at rest - A bifocal TMS study. *Clinical Neurophysiology*, **120**(9), 1724–1731.

Bencivenga, F., Sulpizio, V., Tullo, M. G., & Galati, G. (2021). Assessing the effective connectivity of premotor areas during real vs imagined grasping: A DCM-PEB approach. *Neuroimage*, **230**, 117806.

De Beukelaar, T. T., Alaerts, K., Swinnen, S. P., & Wenderoth, N. (2016). Motor facilitation during action observation : The role of M1 and PMv in grasp predictions. *Cortex; A Journal Devoted to the Study of the Nervous System and Behavior*, **75**, 180–192.

Buch, E. R., Johnen, V. M., Nelissen, N., O'Shea, J., & Rushworth, M. F. S. (2011). Noninvasive associative plasticity induction in a corticocortical pathway of the human brain. *Journal of Neuroscience*, **31**(48), 17669–17679.

Cardellicchio, P., Koch, G., Fadiga, L., & D'Ausilio, A. (2021). Motor overload: GABAergic index of parallel buffer costs. *Brain Stimulation*, **14**(5), 1106–1108.

Cattaneo, L., Voss, M., Brochier, T., Prabhu, G., Wolpert, D. M., & Lemon, R. N. (2005). A cortico-cortical mechanism mediating object-driven grasp in humans. *PNAS*, **102**(3), 898–903.

Cerri, G., Shimazu, H., Maier, M. A., & Lemon, R. N. (2003). Facilitation from ventral premotor cortex of primary motor cortex outputs to macaque hand muscles. *Journal of Neurophysiology*, **90**(2), 832–842.

Davare, M., Lemon, R. &., & Olivier, E. (2008). Selective modulation of interactions between ventral premotor cortex and primary motor cortex during precision grasping in humans. *Journal of Physiology*, **586**(11), 2735–2742.

Davare, M., Montague, K., Olivier, E., Rothwell, J. C., & Lemon, R. N. (2009). Ventral premotor to primary motor cortical interactions during object-driven grasp in humans. *Cortex; A Journal Devoted to the Study of the Nervous System and Behavior*, **45**(9), 1050–1057.

Davare, M., Rothwell, J. C., & Lemon, R. N. (2010). Causal connectivity between the human anterior intraparietal area and premotor cortex during grasp. *Current Biology*, **20**(2), 176–181.

Derosiere, G., Vassiliadis, P., & Duque, J. (2020). Advanced TMS approaches to probe corticospinal excitability during action preparation. *Neuroimage*, **213**, 116746.

Dutar, P., & Nicoll, R. A. (1988). A physiological rpòe for GABAB receptors in the central nervous system. *Nature*, **332**(6160), 156–158.

Federico, P., & Perez, M. A. (2017). Distinct corticocortical contributions to human precision and power grip. *Cerebral Cortex*, **27**(11), 5070–5082.

Fiori, F., Chiappini, E., & Avenanti, A. (2018). Enhanced action performance following TMS manipulation of associative plasticity in ventral premotor-motor pathway. *Neuroimage*, **183**, 847–858.

Fisher, R. J., Nakamura, Y., Bestmann, S., Rothwell, J. C., & Bostock, H. (2002). Two phases of intracortical inhibition revealed by transcranial magnetic threshold tracking. *Experimental Brain Research*, **143**(2), 240–248.

Fogassi, L., Gallese, V., Buccino, G., Craighero, L., Fadiga, L., & Rizzolatti, G. (2001). Cortical mechanism for the visual guidance of hand grasping movements in the monkey: A reversible inactivation study. *Brain*, **124**(3), 571–586.

Fong, P. Y., Spampinato, D., Rocchi, L., Hannah, R., Teng, Y., Di Santo, A., Shoura, M., Bhatia, K., & Rothwell, J. C. (2021). Two forms of short-interval intracortical inhibition in human motor cortex. *Brain Stimulation*, **14**(5), 1340–1352.

Ghosh, B. Y. S., & Porter, R. (1988). Corticocortical synaptic influences on morphologically identified pyramidal neurones in the motor cortex of the monkey. *Journal of Physiology*, **400**(1), 617–629.

Grol, M. J., Majdandžić, J., Stephan, K. E., Verhagen, L., Dijkerman, H. C., Bekkering, H., Verstraten, F. A. J., & Toni, I. (2007). Parieto-frontal connectivity during visually guided grasping. *Journal of Neuroscience*, **27**(44), 11877–11887.

Hamada, M., Galea, J. M., Di Lazzaro, V., Mazzone, P., Ziemann, X. U., & Rothwell, J. C. (2014). Two distinct interneuron circuits in human motor cortex are linked to different subsets of physiological and behavioral plasticity. *Journal of Neuroscience*, **34**(38), 12837–12849.

Hannah, R., Rocchi, L., Tremblay, S., Wilson, E., & Rothwell, J. C. (2020). Pulse width biases the balance of excitation and inhibition recruited by transcranial magnetic stimulation. *Brain Stimulation*, **13**(3), 536–538.

Hebb, D. O. (1949). The Organization of Behavior: A Neuropsychological Theory. *New York Sci Ed*; https://doi.org/10.2307/1418888

Ilić, T. V., Meintzschel, F., Cleff, U., Ruge, D., Kessler, K. R., & Ziemann, U. (2002). Short-interval paired-pulse inhibition and facilitation of human motor cortex: The dimension of stimulus intensity. *Journal of Physiology*, **545**(1), 153–167.

Jiang, X., Wang, G., Lee, A. J., Stornetta, R. L., & Zhu, J. J. (2013). The organization of two new cortical interneuronal circuits. *Nature Neuroscience*, **16**(2), 210–218.

Johnson, M. D., Hyngstrom, A. S., Manuel, M. &., & Heckman, C. J. (2012). Push – Pull control of motor output. *Journal of Neuroscience*, **32**(13), 4592–4599.

Kampa, B. M., Letzkus, J. J., & Stuart, G. J. (2007). Dendritic mechanisms controlling spike-timing-dependent synaptic plasticity. *Trends in Neuroscience (Tins)*, **30**(9), 456–463.

Klein, P. A., Olivier, E., & Duque, J. (2012). Influence of reward on corticospinal excitability during movement preparation. *Journal of Neuroscience*, **32**(50), 18124–18136.

Koch, G., Cercignani, M., Pecchioli, C., Versace, V., Oliveri, M., Caltagirone, C., Rothwell, J., & Bozzali, M. (2010). In vivo definition of parieto-motor connections involved in planning of grasping movements. *Neuroimage*, **51**(1), 300–312.

Koch, G., Ponzo, V., Di Lorenzo, F., Caltagirone, C., & Veniero, D. (2013). Hebbian and anti-Hebbian spike-timing-dependent plasticity of human cortico-cortical connections. *Journal of Neuroscience*, **33**(23), 9725–9733.

Koch, G., Versace, V., Bonnì, S., Lupo, F., Lo, E., Oliveri, M., Caltagirone, C., Unit, S., Neuroscienze, D., Tor, R., & Oxford, V. (2010). Resonance of cortico – cortical connections of the motor system with the observation of goal directed grasping movements. *Neuropsychologia*, **48**(12,), 3513–3520.

Di Lazzaro, V., Pilato, F., Dileone, M., Ranieri, F., Ricci, V., Profice, P., Bria, P., Tonali, P. A., & Ziemann, U. (2006). GABAA receptor subtype specific enhancement of inhibition in human motor cortex. *Journal of Physiology*, **575**(3), 721–726.

Di Lazzaro, V., Pilato, F., Oliviero, A., Dileone, M., Saturno, E., Mazzone, P., Insola, A., Profice, P., Ranieri, F., Capone, F., Tonali, P. A., & Rothwell, J. C. (2006). Origin of facilitation of motor-evoked potentials after paired magnetic stimulation: Direct recording of epidural activity in conscious humans. *Journal of Neurophysiology*, **96**(4,), 1765–1771.

Di Lazzaro, V., Profice, P., Ranieri, F., Capone, F., Dileone, M., Oliviero, A., & Pilato, F. (2012). I-wave origin and modulation. *Brain Stimulation*, **5**(4), 512–525.

Di Lazzaro, V., & Rothwell, J. C. (2014). Corticospinal activity evoked and modulated by non-invasive stimulation of the intact human motor cortex. *Journal of Physiology*, **592**(19), 4115–4128.

Leocani, L., Cohen, L. G., Wassermann, E. M., Ikoma, K., & Hallett, M. (2000). Human corticospinal excitability evaluated with transcranial magnetic stimulation during different reaction time paradigms. *Brain*, **123**(6), 1161–1173.

Markram, H., Gerstner, W., & Sjöström, P. J. (2011). A history of spike-timing-dependent plasticity. *Frontiers in Synaptic Neuroscience*, **3**, 1–24.

McDonnell, M. N., Orekhov, Y., & Ziemann, U. (2006). The role of GABAB receptors in intracortical inhibition in the human motor cortex. *Experimental Brain Research*, **173**(1), 86–93.

Mott, D. D., & Lewis, D. V. (1991). Facilitation of the induction of long-term potentiation by GABAB receptors. *Science (80-)*, **252**(5013), 1718–1720.

Müller-Dahlhaus, J. F. M., Liu, Y., & Ziemann, U. (2008). Inhibitory circuits and the nature of their interactions in the human motor cortex - A pharmacological TMS study. *Journal of Physiology*, **586**(2), 495–514.

Murata, A., Fadiga, L., Fogassi, L., Gallese, V., Raos, V., & Rizzolatti, G. (1997). Object representation in the ventral premotor cortex (Area F5) of the monkey. *Journal of Neurophysiology*, **78**(4), 2226–2230.

Murata, A., Gallese, V., Luppino, G., Kaseda, M., & Sakata, H. (2000). Selectivity for the shape, size, and orientation of objects for grasping in neurons of monkey parietal area AIP. *Journal of Neurophysiology*, **83**(5), 2580–2601.

Ni, Z., Charab, S., Gunraj, C., Nelson, A. J., Udupa, K., Yeh, I. J., & Chen, R. (2011a). Transcranial magnetic stimulation in different current directions activates separate cortical circuits. *Journal of Neurophysiology*, **105**(2), 749–756.

Ni, Z., Gunraj, C., Wagle-Shukla, A., Udupa, K., Mazzella, F., Lozano, A. M., & Chen, R. (2011). Direct demonstration of inhibitory interactions between long interval intracortical inhibition and short interval intracortical inhibition. *Journal of Physiology*, **589**(12), 2955–2962.

Pauly, M. G., Barlage, M., Hamami, F., Steinhardt, J., Baarbé, J., Tran, S., Hanssen, H., Herzog, R., Tadic, V., Brüggemann, N., Chen, R., Münchau, A., Bäumer, T., & Weissbach, A. (2022). Subthalamic nucleus conditioning reduces premotor-motor interaction in Parkinson's disease. *Parkinsonism & Related Disorders*, **96**, 6–12.

Poole, B. J., Mather, M., Livesey, E. J., Harris, I. M., & Harris, J. A. (2018). Motor-evoked potentials reveal functional differences between dominant and non-dominant motor cortices during response preparation. *Cortex; A Journal Devoted to the Study of the Nervous System and Behavior*, **103**, 1–12.

Raos, V., Umiltá, M. A., Murata, A., Fogassi, L., & Gallese, V. (2006). Functional properties of grasping-related neurons in the ventral premotor area F5 of the macaque monkey. *Journal of Neurophysiology*, **95**(2), 709–729.

Roshan, L., Paradiso, G. O., & Chen, R. (2003). Two phases of short-interval intracortical inhibition. *Experimental Brain Research*, **151**(3), 330–337.

Rossi, S., Hallett, M., Rossini, P. M., & Pascual-Leone, A., & Safety of TMS Consensus Group (2009). Safety, ethical considerations, and application guidelines for the use of transcranial magnetic stimulation in clinical practice and research. *Clinical Neurophysiology*, **120**(12), 2008–2039.

Rossini, P. M., Burke, D., Chen, R., Cohen, L. G., Daskalakis, Z., Di Iorio, R., Di Lazzaro, V., Ferreri, F., Fitzgerald, P. B., George, M. S., Hallett, M., Lefaucheur, J. P., Langguth, B., Matsumoto, H., Miniussi, C., Nitsche, M. A., Pascual-Leone, A., Paulus, W., Rossi, S., …, & Ziemann, U. (2015). Non-invasive electrical and magnetic stimulation of the brain, spinal cord, roots and peripheral nerves: Basic principles and procedures for routine clinical and research application: An updated report from an I.F.C.N. Committee. *Clinical Neurophysiology*, **126**(6), 1071–1107.

Sanchez-Vives, M. V., Barbero-Castillo, A., Perez-Zabalza, M., & Reig, R. (2021). GABAB receptors: Modulation of thalamocortical dynamics and synaptic plasticity. *Neuroscience*, **456**, 131–142.

Schwenkreis, P., Liepert, J., Witscher, K., Fischer, W., Weiller, C., Malin, J. P., & Tegenthoff, M. (2000). Riluzole suppresses motor cortex facilitation in correlation to its plasma level. A study using transcranial magnetic stimulation. *Experimental Brain Research*, **135**(3), 293–299.

Shimazu, H., Maier, M. A., Cerri, G., Kirkwood, P. A., & Lemon, R. N. (2004). Macaque ventral premotor cortex exerts powerful facilitation of motor cortex outputs to upper limb motoneurons. *Journal of Neuroscience*, **24**(5), 1200–1211.

Sjöström, P. J., & Häusser, M. (2006). A cooperative switch determines the sign of synaptic plasticity in distal dendrites of neocortical pyramidal neurons. *Neuron*, **51**(2), 227–238.

Sommer, M., Norden, C., Schmack, L., Rothkegel, H., Lang, N., & Paulus, W. (2013). Opposite optimal current flow directions for induction of neuroplasticity and excitation threshold in the human motor cortex. *Brain Stimulation*, **6**(3), 363–370.

Turella, L., & Lingnau, A. (2014). Neural correlates of grasping. *Frontiers in Human Neuroscience*, **8**, 1–8.

Umilta, M. A., Brochier, T., Spinks, R. L., & Lemon, R. N. (2007). Simultaneous recording of macaque premotor and primary motor cortex neuronal populations reveals different functional contributions to visuomotor grasp. *Journal of Neurophysiology*, **98**(1), 488–501.

Veniero, D., Ponzo, V., & Koch, G. (2013). Paired associative stimulation enforces the communication between interconnected areas. *Journal of Neuroscience*, **33**(34), 13773–13783.

Vucic, S., Cheah, B. C., & Kiernan, M. C. (2011). Dissecting the mechanisms underlying short-interval intracortical inhibition using exercise. *Cerebral Cortex*, **21**(7), 1639–1644.

Werhahn, K. J., Kunesch, E., Noachtar, S., Benecke, R., & Classen, J. (1999). Differential effects on motorcortical inhibition induced by blockade of GABA uptake in humans. *Journal of Physiology*, **517**(2), 591–597.

Ziemann, U. (2020). I-waves in motor cortex revisited. *Experimental Brain Research*, **238**(7–8), 1601–1610.

Ziemann, U., Chen, R., Cohen, L. G., & Hallett, M. (1998). Dextromethorphan decreases the excitability of the human motor cortex. *Neurology*, **51**(5), 1320–1324.

Ziemann, U., Lönnecker, S., Steinhoff, B. J., & Paulus, W. (1996). The effect of lorazepam on the motor cortical excitability in man. *Experimental Brain Research*, **109**(1), 127–135.

Ziemann, U., Reis, J., Schwenkreis, P., Rosanova, M., Strafella, A., Badawy, R., & Müller-Dahlhaus, F. (2015). TMS and drugs revisited 2014. *Clinical Neurophysiology*, **126**(10), 1847–1868.

Ziemann, U., Rothwell, J. C., & Ridding, M. C. (1996). Interaction between intracortical inhibition and facilitation in human motor cortex. *Journal of Physiology*, **496**(3), 873–881.

Additional information

Data availability statement

Data from this study will be made available to qualified investigators upon reasonable request to the corresponding author.

Competing interests

The authors declare that they have no known competing financial interests or personal relationships that could have appeared to influence the work reported in this paper.

Author contributions

A.C.: Conceptualization; Methodology; Software; Data curation; Formal analysis; Investigation; Writing – original draft, Writing – review & editing; Visualization. E.D.: Conceptualization; Methodology; Software; Data curation; Formal analysis; Investigation; Writing – review & editing; Visualization. P.C.: Software; Writing – review & editing. L.F.: Writing – review & editing; Funding acquisition; Resources; Supervision. A.D.: Conceptualization; Methodology; Writing – review & editing; Funding acquisition; Resources; Supervision; Project administration. G.K.: Conceptualization; Methodology; Writing – review & editing; Supervision; Project

administration. All authors read and approved the final version of the manuscript and agree to be accountable for all aspects of the work in ensuring that questions related to the accuracy or integrity of any part of the work are appropriately investigated and resolved. All persons designated as authors qualify for authorship, and all those who qualify for authorship are listed.

Funding

Ministero della Salute (Ministry of Health, Italy): Alessandro D'Ausilio, GR-2018-12 366 027; Ministero della Salute (Ministry of Health, Italy): Alessandro D'Ausilio, GR-2016-0 236 1008; Ministero dell'Università e della Ricerca (MUR): Luciano Fadiga, PRIN 2020; European Commission (EC): Luciano Fadiga, FETPROACT-824 160

Acknowledgements

This work was supported by Ministero della Salute, Ricerca Finalizzata 2016 – Giovani Ricercatori (GR-2016-02361008); Ministero della Salute, Ricerca Finalizzata 2018 – Giovani Ricercatori (GR-2018-12366027) to A.D., and by Ministero dell'Università e della Ricerca – PRIN 2020 – and the European Union H2020 – EnTimeMent (FETPROACT-824160) to L.F. The funders had no role in study design, data collection and analysis, decision to publish, or preparation of the manuscript.

Keywords

cortico-cortical paired associative stimulation, Hebbian-like plasticity, I-waves, LTP-like and LTD-like after-effect, primary motor cortex, ventral premotor cortex

Supporting information

Additional supporting information can be found online in the Supporting Information section at the end of the HTML view of the article. Supporting information files available:

Statistical Summary Document
Peer Review History